AJNR

MR volumetric analysis of the human entorhinal, perirhinal, and temporopolar cortices.

R Insausti, K Juottonen, H Soininen, A M Insausti, K Partanen, P Vainio, M P Laakso and A Pitkänen

AJNR Am J Neuroradiol 1998, 19 (4) 659-671
http://www.ajnr.org/content/19/4/659

AJNR Am J Neuroradiol 19:659–671, April 1998

MR Volumetric Analysis of the Human Entorhinal, Perirhinal, and Temporopolar Cortices

Ricardo Insausti, Kirsi Juottonen, Hilkka Soininen, Ana Maria Insausti, Kaarina Partanen, Pauli Vainio, Mikko P. Laakso, and Asla Pitkänen

PURPOSE: **Our purpose was to investigate the normal volumes of the human entorhinal, perirhinal, and temporopolar cortices on MR imaging studies using a customized program.**

METHODS: **We designed a protocol in which the volumes of the entorhinal, perirhinal, and temporopolar cortices were determined from coronal MR images using anatomic landmarks defined on the basis of cytoarchitectonic analyses of 49 autopsy cases. MR volumetry of these cortical areas was performed in 52 healthy volunteers.**

RESULTS: **The overall mean volumes were 1768 ± 328 mm^3/1558 ± 341 mm^3 (right/left) for the entorhinal cortex, 2512 ± 672 mm^3/2572 ± 666 mm^3 for the perirhinal cortex, and 2960 ± 623 mm^3/3091 ± 636 mm^3 for the temporopolar cortex. The right entorhinal cortex was 12% larger than the left. The volume of the temporopolar cortex was reduced bilaterally by 13% in the older age group compared with younger subjects, while the volumes of the entorhinal and perirhinal cortices were unaffected by age. There were no differences between men and women in the volumes of any of the three cortices.**

CONCLUSION: **Our method provides a tool by which to measure volumes of the entorhinal, perirhinal, and temporopolar cortices on coronal MR images.**

The medial temporal lobe in primates is composed of the amygdala, the hippocampus, and surrounding cortical areas, including the entorhinal, perirhinal, and parahippocampal cortices. These structures are interconnected by a myriad of topographically organized connections (1, 2). Consequently, they function in concert when guiding the performance of complex behavioral tasks, such as formation of memories (3). It has long been believed that the hippocampus is the most critical component of the medial temporal lobe memory system. However, it has been found that damage to the entorhinal and perirhinal cortices can also cause memory impairment (4–7). Nevertheless, the contribution of these cortical areas to memory processing in humans has remained obscure, in part owing to the difficulties in defining and quantifying these regions in the brains of living, awake humans.

Most of the parahippocampal gyrus is occupied by the entorhinal area (area 28 of Brodmann) (8) that is bordered dorsomedially by the periamygdaloid cortex and caudomedially by the presubiculum and parasubiculum. Laterally, it extends to the medial bank of the collateral sulcus, where it is bordered by the perirhinal cortex laterally (9). The perirhinal cortex may be divided into several cytoarchitectonically distinct subfields (8, 10, 11). Area 35 of the perirhinal cortex follows the collateral sulcus along its full rostrocaudal extent and occupies chiefly the fundus and the medial bank of the sulcus. Most of the perirhinal cortex is composed of area 36, which lies medial to area TE (12) (also called area 20 by Brodmann) (8). Anteriorly, the perirhinal cortex is continuous with the rostralmost portion of the temporal pole (area TG of von Bonin and Bailey [12]; area 38 of Brodmann [8]).

MR-based volumetry has successfully been used in analyses of hippocampal and amygdaloid damage in human diseases, although attempts to define the extent of damage to the entorhinal or perirhinal cortex using MR imaging techniques have been sparse (13). Here, we present a protocol that can be used to

Received July 23, 1997; accepted after revision November 20.

Supported by the Academy of Finland (A.P. and H.S.), by the Sigrid Juselius Foundation (A.P.), by the Vaajasalo Foundation (A.P.), FIS 86/1129, 88/1682, and the Government of Navarra, Department of Health projects (R.I).

Presented in part at the annual meeting of the American Society for Neurosciences.

From the Department of Anatomy, University of Navarra, Pamplona, Spain (R.I., A.M.I.); and the Departments of Neuroscience and Neurology (K.J., H.S., M.P.L.), Neurology (H.S.), and Radiology (K.P., P.V.), and the A.I. Virtanen Institute (A.P.), University of Kuopio, Finland.

Address reprint requests to Asla Pitkänen, MD, PhD, A.I. Virtanen Institute, University of Kuopio, P.O. Box 1627, FIN-70 211, Kuopio, Finland.

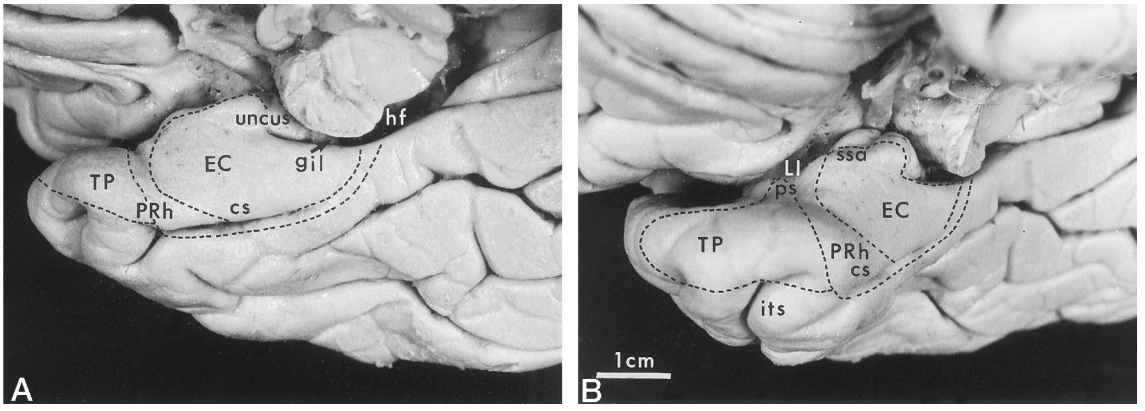

FIG 1. Views of the ventral aspect of the brain show location of entorhinal, perirhinal, and temporopolar cortices. *A* is the ventromedial view and *B* is the frontal view of the temporal lobe. cs = collateral sulcus, EC = entorhinal cortex, gil = gyrus intralimbicus, hf = hippocampal fissure, its = inferior temporal sulcus, LI = limen insulae, PRh = perirhinal cortex, ps = temporopolar sulcus, ssa = sulcus semiannularis, TP = temporopolar cortex.

identify the entorhinal and perirhinal cortices as well as the associated temporopolar cortex on coronal MR images in order to obtain MR-based volumetric measurements.

Methods

Subjects and Tissue Preparation for Histology

Forty-four brains from autopsies were available for histologic analysis (23 men and 21 women; mean age, 55 ± 24 years; range, 12 to 110 years). The right hemisphere was analyzed in 27 cases and the left in 17 cases. No differences were observed in the lamination, subfields, or topographic relationships of various cortical areas between the left and right hemispheres. All brains were examined by a neuropathologist to exclude any cerebral diseases that might complicate the identification of the cytoarchitectonic boundaries of the cortical areas.

Protocols for fixation, cryoprotection, cutting, and storage of human brain tissue were carried out as described previously by Insausti et al (9). For cytoarchitectonic analysis, a one-in-eight or one-in-10 series of sections (50-μm thick), including the entire rostrocaudal extent of the temporopolar, perirhinal, and entorhinal cortices, was stained with thionin. In approximately half the cases, a series of coronal sections was cut perpendicular to the line drawn between the anterior and posterior commissures. This plane of sectioning was in accord with that in the coronal MR images, which facilitated the transposition of the histologic boundaries onto the MR images.

MR Imaging

Subjects for MR Imaging.—Fifty-two healthy subjects (22 men, 30 women) were included in this study. Their mean age was 55 ± 22 years (range, 21 to 79 years). Younger control subjects (n = 20; mean age, 28 ± 7 years) were interviewed by a neurologist to exclude the presence of any diseases involving the CNS. The older control subjects (n = 32; mean age, 72 ± 4 years) underwent a general physical examination, a clinical neurologic examination, extensive neuropsychological testing, electroencephalography, event-related potentials, and MR imaging (for details, see Soininen et al [14]). As in previous studies, their memory and other cognitive functions were normal (14).

MR Image Acquisition.—The subjects were scanned with a 1.5-T imager using a standard head coil and a tilted coronal 3-D magnetization-prepared rapid acquisition gradient-echo (MP-RAGE) sequence with parameters of 10/4/1 (TR/TE/excitations); inversion time, 250; flip angle, 12°; field of view, 250 mm; matrix, 256 × 192. This resulted in 128 contiguous T1-weighted partitions with a section thickness of 1.5 to 1.8 mm oriented perpendicular to the long axis of the hippocampus. To adapt the histologic boundaries to determine the borders of the entorhinal and perirhinal cortices on the MR images, partitions throughout the entire rostrocaudal extent of the entorhinal and perirhinal cortices were reconstructed into contiguous sections (2-mm thick) oriented perpendicular to the line drawn between the anterior and posterior commissures at the midsagittal level. For volumetry, the images were magnified and interpolated fourfold, which resulted in an effective pixel size of 0.25 mm. This procedure greatly reduces the error in tracing the boundary of the cortex.

Definition of the Borders of the Entorhinal, Perirhinal, and Temporopolar Cortices on Histologic Sections

The macroscopic location of the temporopolar, perirhinal, and entorhinal cortices in the ventral aspect of the temporal lobe is shown in Figure 1 and their appearance in histologic sections in Figure 2. The following descriptions of the major anatomic landmarks used to identify each of the cortical regions proceed in a rostral to caudal direction.

Although the temporopolar cortex shares some anatomic similarities with the perirhinal cortex (1, 11), and portions of it have in some studies been included with the perirhinal cortex (11), it is commonly considered to be a separate region (8, 12). In the present study, the perirhinal cortex, the area around the collateral sulcus that includes areas 35 and 36 of Brodmann (8, 10, 11), and the temporopolar cortex, which encompasses most of the temporal pole (area TG of von Bonin and Bailey [12] and area 38 of Brodmann [8]), were considered separately. For some statistical analyses, however, their volumes were combined and referred to as the "total perirhinal cortex."

Temporopolar Cortex.—The temporopolar cortex is located rostral to the perirhinal cortex and covers the anterior portion of the temporal lobe. Laterally and ventrolaterally, the temporopolar cortex is surrounded by cortex forming the superior and inferior temporal gyri (Figs 1–4).

In the dorsal aspect of the temporal lobe, the temporopolar sulci extend from the rostral tip of the temporal pole as far caudally as the limen insulae (Figs 2 and 4), although their number and lengths vary. One or two of these sulci may define one or two transverse gyri of Schwalbe (Figs 2B and 4B). In our study, 80% of the cases had two temporopolar sulci, about 12% had a single temporopolar sulcus, and in 8% of the cases the dorsal aspect of the temporal pole was almost completely smooth. The boundary between the temporopolar cortex and the neocortex of the superior temporal gyrus lies at the fundus

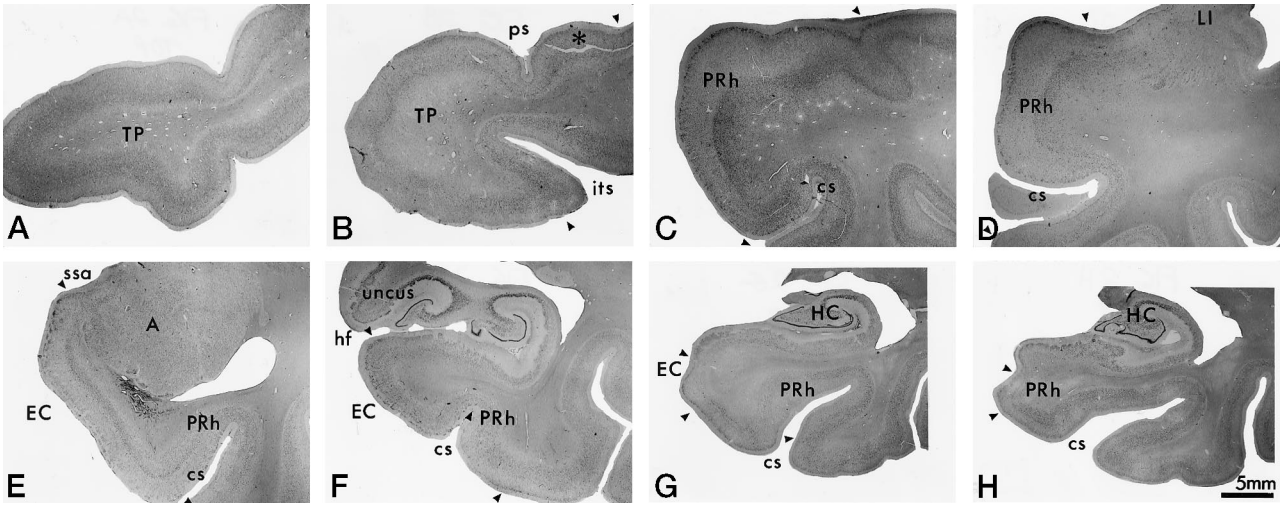

FIG 2. Brightfield photomicrographs of thionin-stained coronal sections show cytoarchitectonic borders (indicated with *arrowheads*) of the temporopolar, perirhinal, and entorhinal cortices in four individuals: *A*, 47-year-old man; *B*, 41-year-old woman; *C–F*, 65-year-old man; *G* and *H*, 78-year-old man. Note that in *E* the collateral sulcus is "regular" and in *F* it is "shallow." The sections in *A–F* were chosen from the same eight rostrocaudal levels as the MR images in Figures 3 and 4 (*G* is the last section that contains the entorhinal cortex and *H* is the last section that contains the perirhinal cortex). A = amygdala, cs = collateral sulcus, EC = entorhinal cortex, HC = hippocampus, hf = hippocampal fissure, its = inferior temporal sulcus, LI = limen insulae, ps = temporopolar sulcus, PRh = perirhinal cortex, ssa = sulcus semiannularis, TP = temporal pole; *asterisk* indicates the gyrus of Schwalbe.

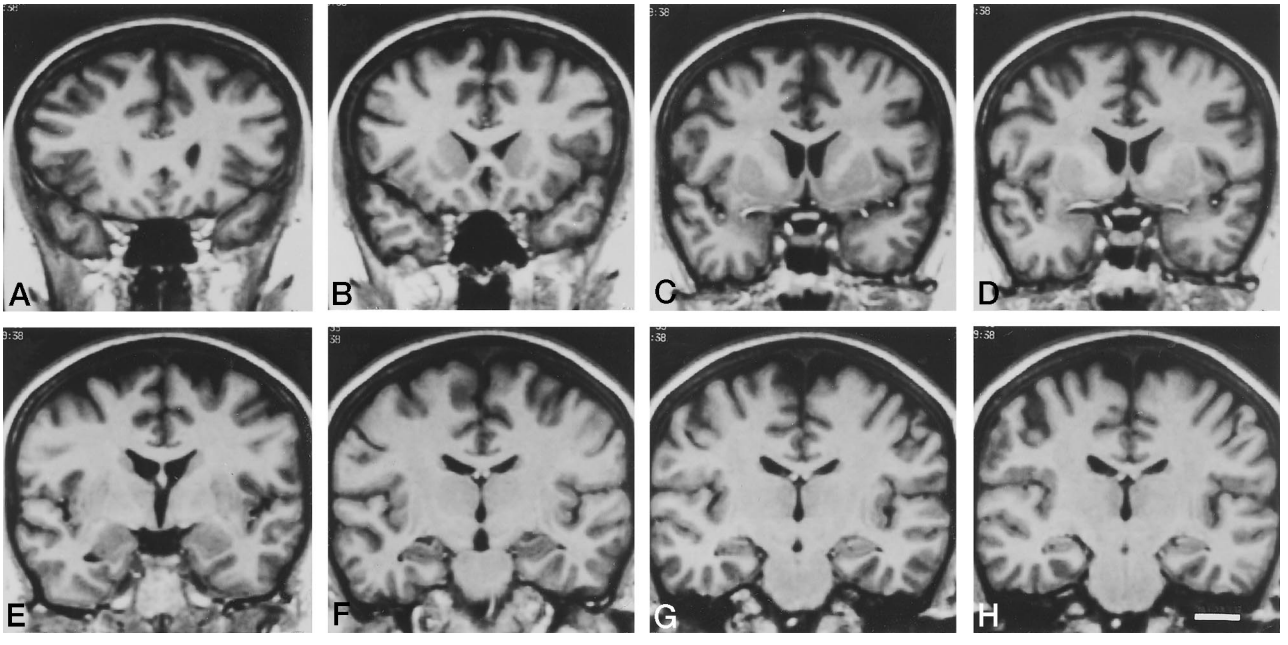

FIG 3. Coronal MR images in a 43-year-old woman taken from eight rostrocaudal levels, from which the higher-magnification images shown in Figure 4 were enlarged. *A* is the most rostral and *H* is the most caudal. Scale bar (in *H*) = 20 mm.

or within the lateral bank of the lateral polar sulcus (Figs 2 and 4–6) (12). Our histologic analysis revealed that, at approximately midlevel of its rostrocaudal extent, the temporopolar cortex typically extends beyond the lateral bank of the lateral temporopolar sulcus on average by 8 mm (range, 5 to 14 mm). This mismatch between the histologic boundary and the sulcal landmark, however, was usually present only at the one level (corresponding to the MR level in Fig 4B and C), and therefore had little effect on the total volume of the temporopolar cortex. Obviously, this cytoarchitectonic variation was not detectable on the MR images.

Ventrally, the transition between the temporopolar cortex and the inferotemporal cortex in most of the histologic cases occurred at the lateral edge of the superior temporal sulcus and, when the inferior temporal sulcus appeared, at its lateral edge (Figs 2, 4, and 5). The superior and inferior temporal sulci define the boundary caudal to the level at which the collateral sulcus appears. One of the major factors causing variability in our volumetric analyses both on histologic sections and on MR images was the large variation between individuals in the location, extent, and shape of the rostral tips of the superior and inferior temporal sulci, which determine the ventrolateral border of the temporopolar cortex. For example, the shape of the anterior end of the superior temporal sulcus depends on the position of the temporal bone in the middle cranial fossa, the overall shape of the brain, the length of the sulci along the temporal lobe, and the head position during MR imaging. For MR volumetry, we determined that the most reproducible

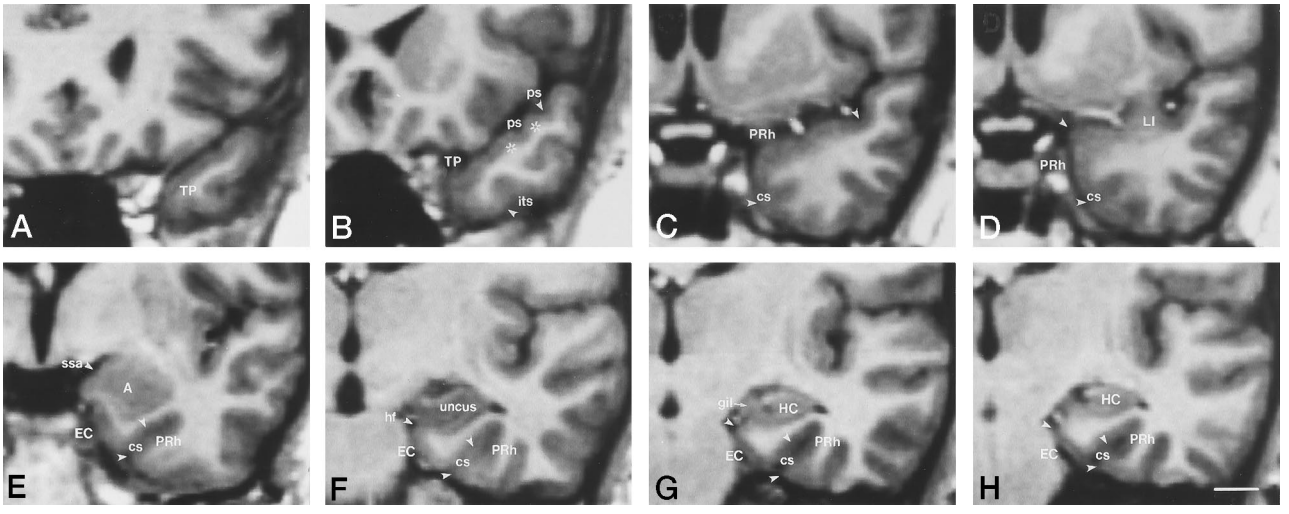

FIG 4. Major anatomic landmarks used to identify the temporopolar, perirhinal, and entorhinal cortical boundaries (indicated with *arrowheads*) in coronal MR images. *A* is the most rostral and *H* is the most caudal.

A, The entire cortex in this view is part of the temporopolar cortex (TP).

B, In the dorsal aspect of the brain, the fundus of the more lateral temporopolar sulcus (ps) defines the dorsolateral border of the temporopolar cortex. The two gyri of Schwalbe are indicated with *asterisks*. In the ventral aspect of the brain, the temporopolar cortex extends to the lateral edge of the inferior temporal sulcus (its).

C, Caudally, the collateral sulcus (cs) appears in the ventromedial aspect of the brain, and the rostral extent of the perirhinal cortex (PRh) is apparent. Dorsally, the fundus of the temporopolar sulcus forms the lateral border of the perirhinal cortex, and its ventral border is at the lateral border of the lateral bank of the collateral sulcus.

D, MR image at the level of the limen insulae (LI). The perirhinal cortex is the region between the midpoint of the parahippocampal gyrus and the lateral border of the lateral bank of the collateral sulcus.

E, MR image at the level of the amygdala. The fundus of the sulcus semiannularis (ssa) defines the dorsal border of the entorhinal cortex (EC). Because the collateral sulcus is regular (depth between 1 and 1.5 cm), the lateral border of the entorhinal cortex is located at the midpoint of the medial bank of the collateral sulcus. The lateral border of the perirhinal cortex is at the edge of the lateral bank of the collateral sulcus. The inferotemporal cortex is lateral to the perirhinal cortex.

F, At the uncal level, the entorhinal cortex extends medially to the hippocampal fissure (hf) and laterally to the midpoint of the medial bank of the collateral sulcus. The lateral border of the perirhinal cortex is at the lateral edge of the lateral bank of the collateral sulcus.

G, At the level of the gyrus intralimbicus (gil), the entorhinal cortex extends from the hippocampal fissure to the midpoint of the medial bank of the collateral sulcus. The medial and lateral borders of the perirhinal cortex is as in *F*.

H, MR image caudal to the gyrus intralimbicus. This is the last section that contains the entorhinal cortex, and the perirhinal cortex extends one more section caudally. Scale bar = 10 mm.

location for the ventrolateral border of the temporal pole was at the lateral edge of the superior or inferior temporal sulci.

As for the most rostral portion of the temporal lobe, cytoarchitectonic analyses showed that the neocortex of the superior temporal gyrus extends as far rostrally as the superior temporal sulcus. More anteriorly, the entire temporal pole belongs cytoarchitectonically to the temporopolar cortex (Fig 2A). Therefore, the rostral tip of the temporal pole is made up of a cytoarchitectonically homogeneous cortex. Usually, this region covers approximately 6 to 8 mm of the rostral pole of the temporal lobe, regardless of the shape and number of sulci. However, its size varies among individuals and depends on the morphology of the superior temporal sulcus.

Perirhinal Cortex.—The perirhinal cortex borders the temporopolar cortex along the medial surface of the rostral temporal lobe. Rostrally, the perirhinal cortex replaces the temporopolar cortex in the dorsomedial aspect of the temporal lobe, and, caudally, in the ventromedial temporal lobe as well. At more caudal levels, the perirhinal cortex surrounds all but the most medial aspect of the entorhinal cortex (Fig 2).

The limen insulae proved to be a useful landmark in identifying the beginning of the perirhinal cortex in human brain, the rostral tip of which lies a few millimeters anterior to the limen insulae (Figs 2, 4, and 5). Based on measurements from our histologic series, this level is on average 24 mm caudal to the temporal pole (range, 18 to 28 mm). Another useful landmark was the rostral end of the collateral sulcus, where the temporopolar cortex was replaced by the perirhinal cortex in most cases (Figs 2 and 4). The mean distance between the anterior end of the perirhinal cortex and the rostral tip of the collateral sulcus was 0 mm (range, ± 2 mm). However, we would like to point out that the collateral sulcus has a highly variable shape and length and may be asymmetric in the left and right hemispheres (9).

Throughout its rostrocaudal extent, the perirhinal cortex is bordered laterally by the neocortex of the inferior temporal gyrus (Figs 2 and 4) (area 20 of Brodmann [8]; area TE of von Bonin and Bailey [12]). Hereafter, this cortical area will be referred to as the inferotemporal cortex. The transition from the perirhinal cortex to the inferotemporal cortex usually occurs within the lateral bank of the collateral sulcus. The location of the border between the perirhinal and inferotemporal cortices depends on the depth of the collateral sulcus (Figs 7 and 8). In 82% of the cases, the collateral sulcus was "regular" (depth between 1 and 1.5 cm) and the cytoarchitectonic border between the perirhinal and inferotemporal cortices was at the lateral edge of the collateral sulcus. Less often (16%) the sulcus was "shallow" (depth < 1 cm), or it had shallow segments, sometimes even interruptions, along its rostrocaudal extent. In these cases, the perirhinal cortex extended up to the midpoint of the occipitotemporal gyrus (also known as the fusiform gyrus). In rare cases (2%), the sulcus was "deep" (depth ≥ 1.5 cm), causing the border to lie within the lateral bank of the collateral sulcus, usually at its midpoint. Medially, the perirhinal cortex borders the entorhinal cortex, the boundary of which is described below.

The caudal limit of the perirhinal cortex can be identified by using the end of the entorhinal cortex (level of the gyrus intralimbicus) as a landmark. At this level, the width of the entorhinal cortex decreases dramatically within a short distance

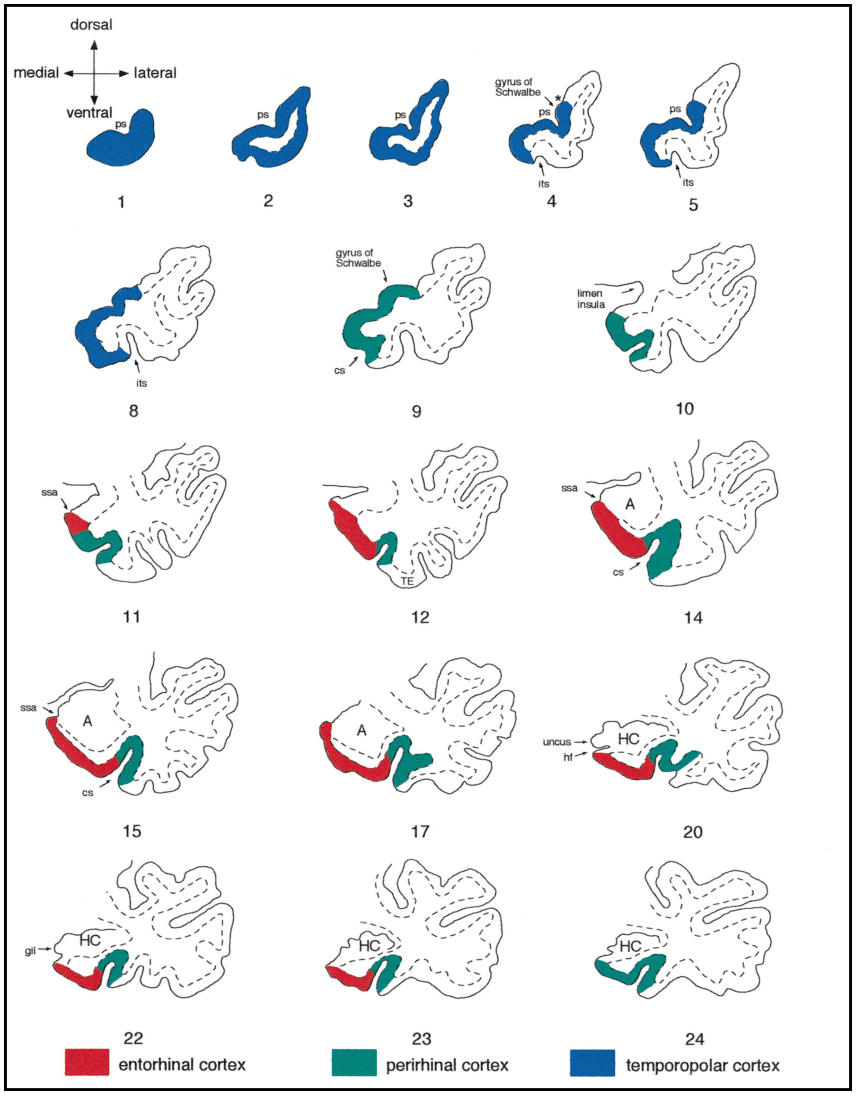

FIG 5. Schematic drawings summarize the anatomic landmarks used to draw the outlines of the temporopolar, perirhinal, and entorhinal cortices on coronal MR images. Sections were outlined from a series of 2-mm-thick coronal MR images from one healthy subject (section numbers 1–24). Only the MR images displaying critical landmarks are shown (therefore, some section numbers are missing). *Red* indicates the entorhinal cortex, *green* the perirhinal cortex, and *blue* the temporopolar cortex. Note that in section 4, the temporopolar cortex recedes and the superior temporal gyrus and inferotemporal cortex appear associated with the most rostral portions of the superior temporal sulcus (sts) and the inferior temporal sulcus (its), respectively. A single temporopolar sulcus (ps) is present in the first five sections, the lateral edge of which demarcates the dorsal limit of the temporopolar cortex (*asterisk*). The appearance of the collateral sulcus (cs) in section 9 marks the transition between the temporopolar and perirhinal cortices (the latter shown in *green*). At the level of the limen insulae in section 10, the dorsomedial border of the perirhinal cortex is at the most medial point of the parahippocampal gyrus (note that we have included the piriform cortex into the perirhinal cortex). Section 11 (one section behind the limen insulae) marks the beginning of the entorhinal cortex (*red*), which extends medially to the sulcus semiannularis (ssa). In this case, the depth of the collateral sulcus is regular, and therefore, the border between the entorhinal and perirhinal cortices is at the midpoint of the medial bank of the collateral sulcus. The boundary between the perirhinal and inferotemporal (TE) cortices is at the lateral edge of the sulcus. Note how in sections 17 and 20, a small gyrus appears in the depth of the collateral sulcus owing to its noncontinuous course. These interruptions can most often be detected at the level of the uncus. The gyrus intralimbicus (gil) located at the caudal end of the uncus can be seen in section 22. Note that the end of the entorhinal cortex is one section behind the end of the uncus (section 23). The perirhinal cortex extends one more section caudally (section 24). A = amygdala, cs = collateral sulcus, its = inferior temporal sulcus, gil = gyrus intralimbicus, HC = hippocampus, hf = hippocampal fissure, ssa = sulcus semiannularis, TE = area TE.

(equivalent to the thickness of one 2-mm MR section). Our histologic analyses revealed that the posterior portion of the perirhinal cortex, while it lacks any distinct gross anatomic landmarks, surrounds the entorhinal cortex caudally for an average distance of 2.9 mm (range, 2 to 4 mm). Consequently, at its most caudal extent, the perirhinal cortex borders the parasubiculum for a short distance (2 to 4 mm) (Fig 2). Thereafter, the perirhinal cortex is replaced by the posterior parahippocampal cortex (areas TH and TF of von Bonin and Bailey [12]). Previous histologic evidence supports our definition of these cytoarchitectonic features (10) (Insausti, unpublished observations).

Entorhinal Cortex.—The cytoarchitectonic characterization of the entorhinal cortex has recently been described (9), and only the anatomic landmarks that are essential for our MR volumetric analyses will be described here. Overall, the entorhinal cortex has several gross anatomic landmarks that make its identification on MR images relatively precise. The rostral extreme of the entorhinal cortex is associated with the appearance of the limen insulae. In our histologic series, the most rostral section containing the entorhinal cortex was on average 2 mm (ie, the thickness of one MR section) behind the limen insulae (range, 0 to 6 mm). At this level, the entorhinal cortex borders with the perirhinal and periamygdaloid cortices (Fig 2), and at times in these sections the rhinal sulcus is also apparent. However, its use as an anatomic landmark in defining the rostromedial border of the entorhinal cortex is of limited value, since the sulcus has a rather vertical orientation and a variable shape, making its detection on coronal MR images difficult. Moreover, our histologic analyses showed little correlation between the appearance of the rhinal sulcus and the rostral limit of the entorhinal cortex. A more reliable landmark in identifying the medial border of the entorhinal cortex is the ventral border of the gyrus semilunaris, that is, the fundus of the sulcus semiannularis (Fig 2E). It was present in all histologic cases and can be readily detected on coronal MR images as well (Fig 4E). The medial portion of the entorhinal cortex forms the gyrus ambiens, which extends caudally to the anterior limit of the hippocampal fissure (Fig 2). The ventral limit of the gyrus

ambiens is marked by a shallow sulcus (the intrarhinal sulcus) (9, 10).

The rostrocaudal midpoint of the entorhinal cortex is at the level of the hippocampal fissure (the choroid fissure), dorsal of which lie the gyrus uncinatus, the band of Giacominni, and the gyrus intralimbicus. Caudomedially, the entorhinal cortex borders the hippocampal fissure, which contains the presubiculum and parasubiculum in its ventral lip (Fig 2), where occasionally the entorhinal cortex itself may also be found. Caudally, the entorhinal cortex blends with the presubiculum and parasubiculum, making identification of its caudal limit somewhat difficult. In our histologic series, the end of the entorhinal cortex was located 1.1 mm (range, +4 mm to −2 mm) behind the section containing the caudalmost portion of the uncus (ie, the gyrus intralimbicus), which is usually clearly visible on coronal MR images.

Laterally, the entorhinal cortex usually extends to the medial bank of the collateral sulcus, where it borders the perirhinal cortex (Fig 2). The cytoarchitectonic border between the entorhinal and perirhinal cortices is somewhat variable depending on the depth of the collateral sulcus (Fig 8). If the collateral sulcus is "regular" (between 1 and 1.5 cm in depth), the cytoarchitectonic border between the entorhinal and perirhinal cortex is located within the medial bank of the collateral sulcus. If the collateral sulcus is "shallow" (depth < 1 cm), the cytoarchitectonic border is located in the fundus of the collateral sulcus. If the sulcus is "deep" (depth ≥ 1.5 cm), the entorhinal-perirhinal border is located within the lateral bank of the sulcus. The depth of the collateral sulcus may vary at different rostrocaudal levels of the same brain.

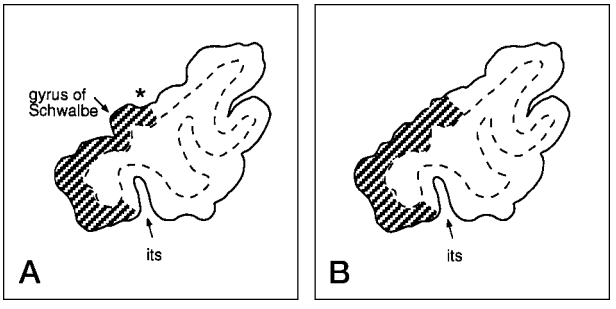

FIG 6. Criteria used to define the dorsolateral border of the temporopolar cortex.

A, When the gyrus of Schwalbe was present, the dorsolateral border of the temporopolar cortex was defined at the lateral border of the gyrus; that is, in the fundus of the temporopolar sulcus (*asterisk*).

B, If the gyrus of Schwalbe was not present, the dorsolateral border of the temporopolar cortex was located at the dorsal midpoint between the medial and lateral corners of the temporal pole. Ventrally, the temporopolar cortex extends to the medial edge of the inferior temporal sulcus (its). The temporopolar cortex is indicated with shading.

Identification of the Borders of the Entorhinal, Perirhinal, and Temporopolar Cortices on Coronal MR Images

According to the histologically defined landmarks, the boundaries of the entorhinal, perirhinal, and temporopolar cortices were drawn manually using a trackball-driven cursor (Figs 3 and 4). These analyses were done by a single investigator, except in cases in which the cortical boundaries were not

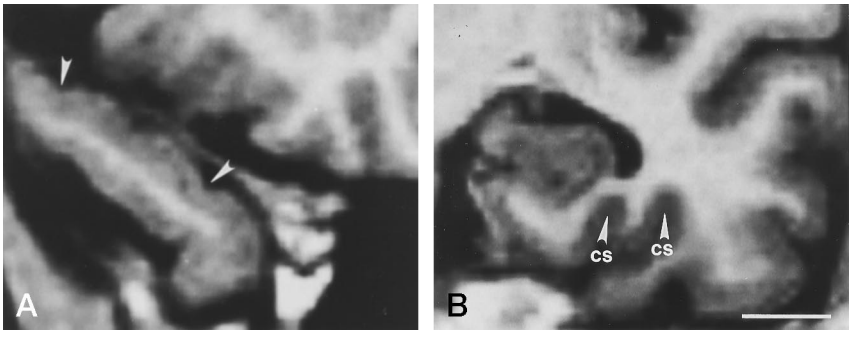

FIG 7. Coronal MR images show two anatomic variations found in the temporal lobe: a transverse gyrus of Schwalbe with two bumps (between *arrowheads*) (*A*) and a divided (ie, extra long) collateral sulcus (cs) (*B*). Scale bar = 10 mm.

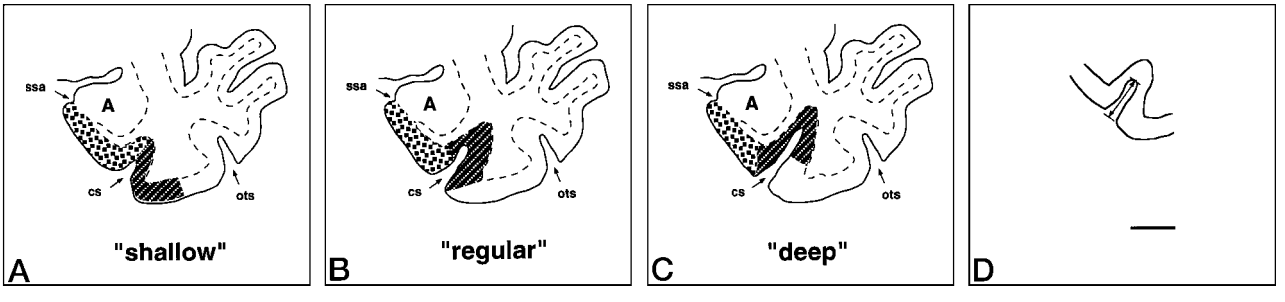

FIG 8. The location of the lateral border of both the entorhinal and perirhinal cortices depends on the depth of the collateral sulcus.

A, A shallow collateral sulcus (depth < 1 cm) is shown. The lateral border of the entorhinal cortex is defined by the fundus of the collateral sulcus. The lateral border of the perirhinal cortex is at the midpoint between the lateral edge of the collateral sulcus and the medial edge of the occipitotemporal sulcus.

B, A regular collateral sulcus (depth between 1 and 1.5 cm) is shown. The lateral border of the entorhinal cortex is at the midpoint of the medial bank of the collateral sulcus. The lateral bank of the perirhinal cortex is at the lateral edge of the collateral sulcus.

C, A deep collateral sulcus (depth ≥ 1.5 cm) is shown. The lateral border of the entorhinal cortex is defined at the medial edge of the collateral sulcus. The lateral border of the perirhinal cortex is at the midpoint between the fundus and the lateral edge of the collateral sulcus.

D, *Arrow* indicates how the depth of the collateral sulcus was measured. cs = collateral sulcus, ots = occipitotemporal sulcus, ssa = sulcus semiannularis. Scale bar = 10 mm.

clear and a second opinion was obtained. The entorhinal, perirhinal, and temporopolar cortical boundaries were outlined from the rostral to caudal direction; that is, outlines of the temporopolar cortex were drawn first, followed by those of the perirhinal and entorhinal cortices. A step-by-step protocol (described below) was used to identify and outline each of the cortical regions on the coronal MR images. To help define the borders of the temporopolar, perirhinal, and entorhinal cortices, the location of these cortical areas relative to the principal landmarks identified on coronal sections is schematically presented in Figure 5.

Step 1.—At the beginning of the analysis, the coronal MR image containing the most rostral portion of the temporal pole (Fig 5, section 1) was selected. The entire cortex in the first three sections (about 6 to 8 mm) was included in the temporopolar cortex. For cases in which the beginning of the superior temporal sulcus or the inferior temporal sulcus was seen within the first three sections, the protocol proceeded to step 3; otherwise, the analysis next followed step 2.

Step 2.—In the fourth section, the temporopolar sulci (and thus the transverse gyri of Schwalbe) usually appeared (Fig 5, section 4), in which case the lateral border of the gyrus (ie, fundus of the small sulcus labeled with an asterisk in Fig 5, section 4) marked the dorsolateral border of the temporopolar cortex (see also Fig 6A). If two temporopolar sulci were present (marked by double gyri of Schwalbe), the dorsolateral border of the temporopolar cortex extended to the bottom of the fundus of the more lateral sulcus (Fig 7A). In some cases there were no temporopolar sulci, such that the dorsal aspect of the temporal pole had a smooth appearance. Here the dorsolateral border of the temporopolar cortex was located at the midpoint of the dorsal aspect of the temporal pole (Fig 6B). The location of the ventrolateral border of the temporopolar cortex depended on whether the superior temporal sulcus and/or the inferior temporal sulcus was present in the section. If either one or both were present, the analysis proceeded to the next step; otherwise, the ventral border of the temporopolar cortex was defined at the midpoint of the ventral aspect of the temporal pole.

Step 3.—When the superior temporal sulcus could be identified (Fig 5, section 4), the ventrolateral border of the temporopolar cortex was located along the medial edge of the superior temporal sulcus. Slightly more caudal, the inferior temporal sulcus appeared (Fig 5, section 5), where, along its medial edge, the lateral border of the temporopolar cortex was defined.

The transition from the temporopolar cortex to the perirhinal cortex was usually observed at the rostral extreme of the collateral sulcus (Fig 5, section 9). Sometimes, however, the collateral sulcus was unusually long and extended as far rostral as the inferior temporal sulcus, indicating that the perirhinal cortex extended that rostrally. In these cases, the identity of the presumed collateral sulcus was made certain in a section in which all five of the temporal lobe gyri could be identified: the superior temporal gyrus, the medial temporal gyrus, the inferior temporal gyrus, the medial occipitotemporal gyrus (also called the fusiform gyrus or the inferotemporal cortex), and the parahippocampal gyrus. Once correctly identified, the collateral sulcus could be accurately followed to its most rostral extent.

Step 4.—The first section containing the perirhinal cortex usually revealed the rostral extreme of the collateral sulcus as well, which was sometimes preceded by the bifurcated white matter in the ventromedial aspect of the temporal lobe (see Fig 5, section 9). Typically, the collateral sulcus appeared one to two sections rostral to the limen insulae (at the level at which the white matter forms a continuum between the frontal and temporal lobes; see Fig 5, section 10). In these cases, the ventrolateral border of the perirhinal cortex was defined at the lateral edge of the collateral sulcus. Sometimes, however, the collateral sulcus was short and did not appear in sections rostral to the limen insulae, yet, based on our histologic analyses, the perirhinal cortex extended rostral to the limen insulae. In these individuals, on the MR section just rostral to the limen insulae, the region of the medial temporal lobe located between the fundus of the most lateral temporopolar sulcus and the medial edge of the inferior temporal sulcus was included with the perirhinal cortex. If the temporopolar sulcus was not present, the dorsal border of the perirhinal cortex was defined at the midpoint of the dorsal aspect of the temporal pole.

Step 5.—On the MR image on which the limen insulae first appeared (Fig 5, section 10), the medial (dorsal) limit of the perirhinal cortex was identified at the most medial point of the parahippocampal gyrus. The lateral border of the perirhinal cortex was delineated by the lateral bank of the collateral sulcus (for variants, see step 7).

Step 6.—The entorhinal cortex was considered to appear one section caudal to the level of the limen insulae. Here, the entorhinal cortex extended from the most medial point of the parahippocampal gyrus to the midpoint of its medial aspect (or an equivalent point if the shape of the parahippocampal gyrus was rounded; see Fig 5, section 1). In more caudal sections in which the sulcus semiannularis was present, the fundus of the sulcus defined the medial limit of the entorhinal cortex. If the sulcus semiannularis was not apparent, the medial extent of the entorhinal cortex was defined at the point where an imaginary extension of the white matter bordering the ventral aspect of the amygdala would touch the pial surface.

Step 7.—The location of the lateral border of the entorhinal cortex depended on the depth of the collateral sulcus (Fig 8). As described above, the collateral sulcus was considered to be shallow if its depth was less than 1 cm, regular if its depth was 1 to 1.4 cm, and deep if its depth was greater than 1.5 cm. Our histologic analyses confirmed that this sulcal depth-dependent adjustment of the entorhinal/perirhinal cortical border was accurate in 94% of the cases.

If the collateral sulcus was shallow, the border between the entorhinal and perirhinal cortices was located at the fundus of the collateral sulcus (Fig 8A), and the border between the perirhinal cortex and area TE was defined by the midpoint between the lateral edge of the collateral sulcus and the medial edge of the occipitotemporal sulcus. If the collateral sulcus was regular, the border between the entorhinal and perirhinal cortices was defined by the midpoint of its medial bank (Fig 8B). In this case, the border between the perirhinal cortex and area TE was identified by the lateral edge of the collateral sulcus (Fig 5, section 12). In the least common cases, in which the collateral sulcus was deep, the border between the entorhinal and perirhinal cortices was located at the medial edge of the collateral sulcus (Fig 8C), and the midpoint of the lateral bank of the collateral sulcus defined the border between the perirhinal cortex and area TE.

Sometimes the collateral sulcus was unusually long or appeared to be divided into two sulci; that is, in some cases (25%) there was a secondary gyrus inside the collateral sulcus on one to three successive MR images (Fig 7B). In these sections, the more medially located collateral sulcus was used to determine the border between the entorhinal and perirhinal cortices. In these cases, the location of the lateral border of the entorhinal cortex varied according to the depth of the sulcus (see above) as if there was only one collateral sulcus. The secondary gyrus, however, influenced the position of the border between the perirhinal and inferotemporal cortices. If the depth of the more medially located collateral sulcus was regular, the border between the perirhinal cortex and area TE was at the fundus of the more laterally situated sulcus. If its depth was shallow, the border was defined by the midpoint between the fundus of the more lateral sulcus and its lateral edge. If the more medial collateral sulcus was deep, the border between the perirhinal cortex and area TE was determined at the midpoint of the secondary gyrus.

Raw volumes of the left and right entorhinal, perirhinal, and temporopolar cortex in the whole control group and in younger and older female and male control subjects.

	Younger Control Subjects			Older Control Subjects		
	All	Women	Men	All	Women	Men
Entorhinal cortex						
Left	1510 ± 271 (1037–2031) (20)	1551 ± 172 (10)	1471 ± 349 (10)	1581 ± 391 (659–2555) (32)	1536 ± 282 (20)	1654 ± 532 (12)
Right	1694 ± 300 (1138–2219) (20)	1669 ± 273 (10)	1719 ± 337 (10)	1802 ± 323 (982–2411) (32)	1844 ± 281 (20)	1734 ± 386 (12)
Perirhinal cortex						
Left	2585 ± 696 (1376–3683) (20)	2616 ± 645 (10)	2555 ± 777 (10)	2254 ± 651 (1054–4144) (32)	2594 ± 751 (20)	2486 ± 462 (12)
Right	2577 ± 865 (1257–4529) (20)	2534 ± 816 (10)	2620 ± 955 (10)	2461 ± 531 (1409–3382) (32)	2513 ± 605 (20)	2374 ± 386 (12)
Temporopolar cortex						
Left	3421 ± 722 (1793–5016) (20)	3364 ± 437 (10)	3479 ± 950 (10)	2894 ± 600 (1535–4237) (32)	2812 ± 549 (20)	3030 ± 681 (12)
Right	3228 ± 703 (1602–4279) (20)	3359 ± 549 (10)	3097 ± 839 (10)	2788 ± 542 (1845–3831) (32)	2784 ± 599 (20)	2793 ± 458 (12)

Note.—Results are presented as a mean ± S.D. (range) (number). The age range for younger control subjects was 21 to 43 years; for older subjects it was 64 to 79 years. All volumes are given in mm^3. Statistical analyses were performed using the raw volumes of the entorhinal and perirhinal cortex and normalized volumes of the temporopolar cortex. MANOVA for repeated measures side × group × gender showed significant effect of group younger vs. older for temporopolar cortex ($F = 8.96$, $P = .004$) and side for the entorhinal cortex ($F = 15.90$, $P = .0001$).

Step 8.—The appearance of the hippocampal fissure (Fig 5, section 20) marks the level at which major changes occur in the shape of the parahippocampal gyrus, including the entorhinal cortex. At the point where the hippocampal fissure could be identified, its location defined the medial border of the entorhinal cortex all the way to its caudal extent. When the hippocampal fissure was not apparent on MR images, the intersection of the pia with the line that forms a continuum with the white matter of the angular bundle was considered to be the medial border of the entorhinal cortex.

Step 9.—The last section showing the gyrus intralimbicus (Fig 5, section 22) was a useful landmark in defining the caudal limits of the entorhinal and perirhinal cortices. The entorhinal cortex ended slightly caudal to (one MR image behind) the posterior limit of the gyrus intralimbicus (Fig 5, section 23), and the perirhinal cortex extended still one more section caudal to the end of the entorhinal cortex. In the last section containing the perirhinal cortex, its medial border was drawn at the point where an imaginary line from the white matter underlying the presubiculum and parasubiculum would extend medially to touch the pial surface. The lateral border of the caudal end of the perirhinal cortex was determined by using the same criteria as described above for its more rostral extent.

Once the entorhinal, perirhinal, and temporopolar cortices were outlined on each of the coronal MR images, volumes for each cortical area were calculated using a program developed in house for a standard work console.

Normalization of the Volumetric Data

It is generally accepted that interindividual variability in head size affects the volumes of various brain regions, including the amygdala and the hippocampus (15). To investigate whether the volumes of the entorhinal, perirhinal, and temporopolar cortices vary with head size, we correlated the raw volumes for each cortical region with the intracranial area measured at the level of the anterior commissure of the same subjects (15). We found a linear relationship between the volume of the temporopolar cortex and the intracranial area ($r = .38$, $P = .006$). Also, the total volume of the perirhinal cortex (ie, the volume of the perirhinal cortex plus the volume of the temporopolar cortex) also correlated with intracranial area ($r = .40$, $P = .004$). Therefore, statistical analyses of the temporopolar cortex or the total perirhinal cortex were performed using both raw and normalized volumes. Normalized cortical area volume was calculated with the formula: (overall mean intracranial area/intracranial area for each subject) × the subject's measured cortical raw volume. Since no correlation was found between the volume of the entorhinal or perirhinal cortices and the intracranial area, only raw values were used in the statistical analyses of these cortices.

Statistical Analyses

The raw and normalized data were analyzed using SPSS software for Windows (version 6.0). Regression analysis was used to calculate the linear relationship between the cortical volumes and intracranial area. We used the multivariate analysis of variance (MANOVA) for repeated measures of side (left, right) × group (younger control subjects, older control subjects) × gender (female × male) comparisons. The results are expressed as the mean ± standard deviation of the mean. The level of statistical significance of differences was set at $P < .05$.

Results

MR Volumetry of the Entorhinal, Perirhinal, and Temporopolar Cortices

General Aspects.—The mean number of 2-mm MR imaging sections comprising the right and left entorhinal cortices was 11.9 (range, 10 to 14) and 11.3 (range, 10 to 13), respectively. The mean number of sections encompassing the right and left perirhinal cortices was 15.1 (range, 13 to 17) and 14.9 (range, 13 to 18), respectively. The right temporopolar cortex extended through an average of 8.0 sections (range, 6 to 10) and the left through an average of 8.3 sections (range, 5 to 10). The average intraobserver variability was 7.4% for the entorhinal cortex, 8.6% for the perirhinal cortex, and 7.3% for the temporopolar cortex. Interobserver variability (10 brains were drawn by two independent investigators) was 12.2% for the entorhinal cortex, 12.2% for the perirhinal cortex, and 11.1% for the temporopolar cortex.

Effects of Age, Sex, and Hemisphere on Cortical Volumes.—The mean volumes of the entorhinal, perirhinal, and temporopolar cortices in younger and older control subjects are presented in the Table.

Figure 9 shows scatterplots of cortical volumes in the regions of interest as a function of age.

Entorhinal cortex. MANOVA for repeated measures of side (right, left) × group × gender comparisons showed no significant reduction in the volume of the entorhinal cortex with age (main effect of group, F = 0.03, P = .862). Neither did we observe any differences in the volume of the entorhinal cortex between males and females (F = 0.00, P = .987) in either age group (gender × group interaction, F = 0.00, P = .990). For the whole study group, the volume of the entorhinal cortex was bigger in the right hemisphere than in the left (F = 15.9, P = .0001). However, there were no interactions between age or gender and side (interaction group × side, F = 0.01, P = .913; gender × side, F = 0.27, P = .606; group × side × gender, F = 3.60, P = .064).

Perirhinal cortex. There was no evidence of a reduction in the volume of the perirhinal cortex with age (F = 0.46, P = .502), and the volumes were similar in both hemispheres (F = 0.27, P = .608) and in both sexes (F = 0.05, P = .830). Neither did we find any significant interactions between group × gender (F = 0.29, P = .590), group × side (F = 0.19, P = .666), gender × side (F = 0.08, P = .778), or group × side × gender (F = 0.19, P = .664).

Temporopolar cortex. There was no evidence of a reduction in the raw volume of the temporopolar cortex as a function of age (F = 1.14, P = .712). However, we did find a reduction in the normalized volume of the temporopolar cortex with age. The mean volume of the right temporopolar cortex was 12% smaller in older control subjects (mean, 2808 mm^3) than in younger control subjects (mean, 3203 mm^3). The mean volume of the left temporopolar cortex was 14% smaller in older control subjects (mean, 2914 mm^3) than in younger control subjects (mean, 3376 mm^3) (main effect of group, F = 8.96, P = .004). There was no effect of gender on raw (F = 0.01, P = .941) or normalized (F = 2.13, P = .151) volumes or of side on raw (F = 3.34, P = .074) or normalized (F = 2.95, P = .092) volumes, or any interactions between group × gender × side.

Combined volumes of the perirhinal and temporopolar cortices. Given the close connectional and functional relationship between the perirhinal and temporopolar cortices, we also calculated the total volume of the perirhinal cortex by combining the volumes of these two cortices. Approximately 45% of the total volume was composed of the perirhinal cortex and 55% was composed of the temporopolar cortex. There was no significant difference in the raw volume of the total perirhinal cortex between the age groups (main effect of group, F = 0.08, P = .784). However, the normalized total volume of the right perirhinal cortex was reduced in older control subjects (mean, 5300 mm^3) by 8% compared with that in younger control subjects (mean, 5747 mm^3), and the total volume of the left perirhinal cortex was reduced by 8% (from 5934 mm^3 to 5494 mm^3) in the older age group (main effect of group, F = 7.59, P = .008). There was no difference in the total raw volume of the perirhinal cortex between males and females (F = 0.06, P = .812), although the normalized volumes were larger in women than in men (F = 5.93, P = .019), a difference that was not dependent on age (interaction group × gender, F = 0.00, P = .978). The total volume of the perirhinal cortex was larger in the left than in the right hemisphere (raw volumes, F = 4.90, P = .032; normalized volumes, F = 4.34, P = .042), a difference that was not dependent on sex (side × gender interaction for raw volumes, F = 1.45, P = .235; for normalized volumes, F = 1.10, P = .301) or age (side × group interaction for raw volumes, F = 0.02, P = .888; for normalized volumes, F = 0.03, P = .862). Similarly, the interaction between group × side × gender was nonsignificant.

Discussion

We describe an MR imaging protocol that can be used to measure the volumes of the human entorhinal, perirhinal, and temporopolar cortices. The landmarks selected to help define the boundaries of the cortical areas on coronal MR images correlate with their gross anatomic and cytoarchitectonic borders on histologic sections. One of the most prominent findings from these analyses was that, unlike the volumes of the entorhinal and perirhinal cortices, the volume of the temporopolar cortex was significantly reduced with age.

Methodological Factors Affecting MR Volumetry

The volumes of the entorhinal, perirhinal, and temporopolar cortices measured by MR imaging varied approximately threefold among subjects, whereas interindividual variability in the volumes of the amygdala and hippocampus has been reported to be approximately twofold (15–17). The variability of volumes when measured directly from histologic sections was twofold for the entorhinal cortex and threefold for the perirhinal cortex (9) (Insausti, unpublished observations). In accord with the present MR imaging data, we observed remarkable interindividual variability in histologic sections in the shape of the sulci that were used to define the borders between the temporopolar cortex and adjacent cortical areas, although in general the sulci and gyri chosen for landmarks still defined the cytoarchitectonic borders reliably. These data suggest that biological variations among individuals explain most of the variability in MR volumetry. Intraobserver and interobserver variability are of minor importance. The criteria used to define the temporopolar cortical borders in the present studies underestimate rather than overestimate its volume, which is a conservative approach to assure that all cortex included in the volumetric analyses lies within the temporal cortical region.

Gross anatomic landmarks were in most cases distinct enough to determine the boundaries of the perirhinal cortex. If the collateral sulcus had a secondary gyrus, most of this "extra" tissue was presumed to belong to the inferotemporal cortex. There-

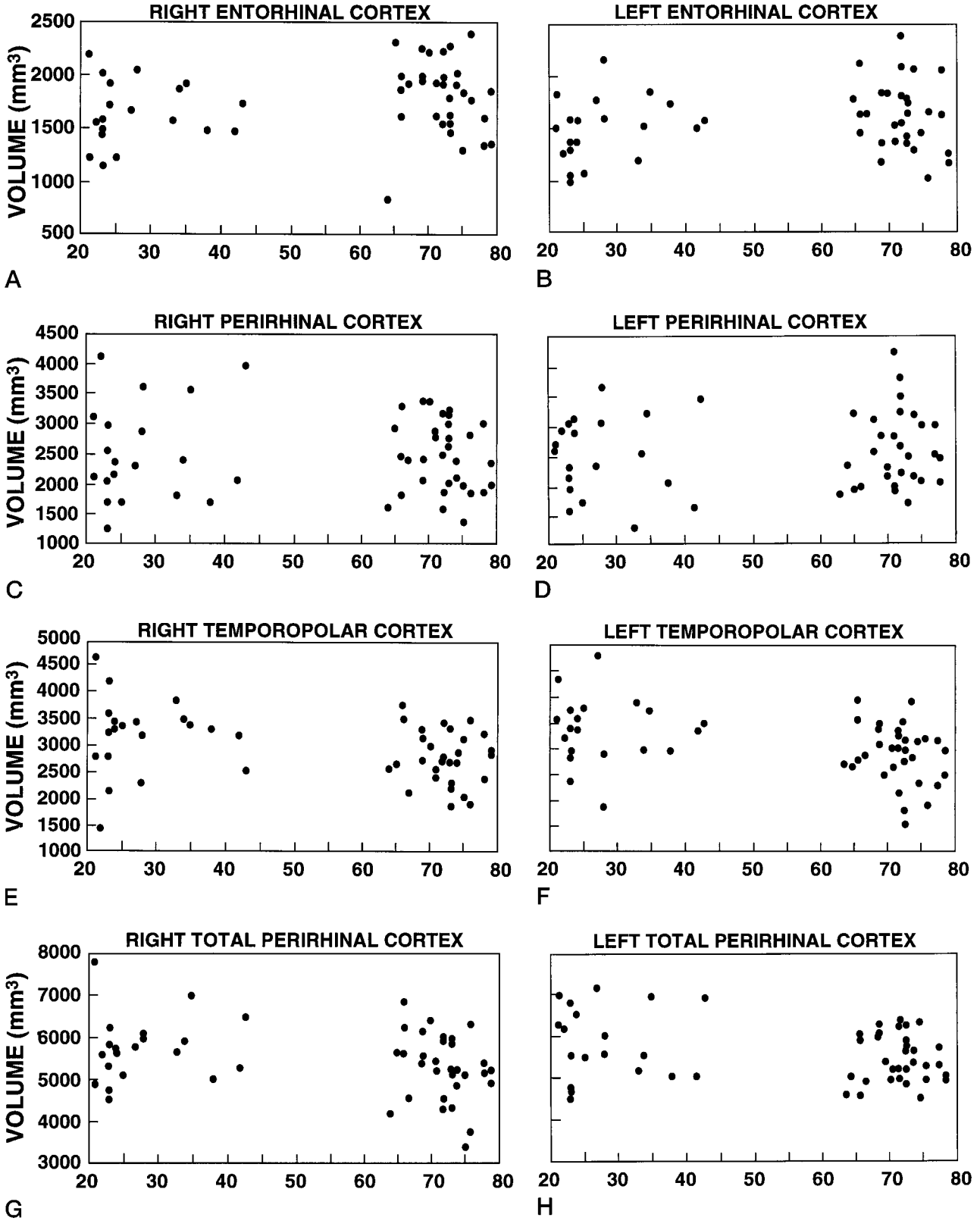

FIG 9. Scatterplots show the effect of age (in years, *horizontal axes*) on the normalized volumes of the entorhinal (*A*, right; *B*, left), perirhinal (*C*, right; *D*, left), temporopolar (*E*, right; *F*, left), and the combined volumes of the perirhinal and temporopolar cortices (the total perirhinal cortex) (*G*, right; *H*, left). There was a main effect of age on the volumes of the temporopolar ($P = .004$) and the total perirhinal ($P = .008$) cortices. We also found a main effect of hemisphere on the volumes of the entorhinal ($P = .001$) and total perirhinal ($P = .042$) cortices. (Statistical analyses were done by repeated MANOVA.)

fore, the more medially located gyrus was used as a reference point for defining the border of the perirhinal cortex. The decision to place the caudal border of the perirhinal cortex one section posterior to the entorhinal cortex was a compromise based on the histologic analyses.

At the level of the limen insulae, the variable shape of the parahippocampal gyrus may hamper definition of the extent of the entorhinal cortex. While this may have caused an underestimation of the volume of the entorhinal cortex at this level, its effect on the total volume of the entorhinal cortex was minimal. At its most caudal end, the width of the entorhinal cortex decreases rapidly, which may result in an overestimation of the entorhinal volume. Yet again, this is restricted to only one MR image through the level caudal to the end of the uncus and would have a minor effect on the entorhinal volume as a whole.

Comparisons of the present data with earlier measurements from other groups is difficult, largely because of differences in cortical border identification or in units used to express absolute or relative volumes. For example, in a study by Pearlson et al (13) volumetric measurements of the entorhinal cortex were made from 3-mm-thick sections that included primarily only the midportion of the entorhinal cortex. Moreover, the cortical areas analyzed in the present study have often been included within the parahippocampal gyrus by others (18–21).

Effect of Age on Cortical Volumes

The temporopolar cortex in older subjects was reduced bilaterally by 13% compared with younger control subjects, which supports a previous MR imaging study by Sullivan et al (17), who found a reduction in temporal lobe gray matter that was associated with normal aging. We did not observe any reduction in the volume of the entorhinal cortex with age, however, which agrees with the findings of Gómez-Isla et al (22), who recently showed that the neuronal number in the entorhinal cortex remained unaffected up to 90 years of age in subjects with no remarkable memory impairment. Nor was there an age-related volume reduction of the perirhinal cortex in our study. These findings differ from those of Convit et al (23), who reported an age-associated decrease in the volume of the fusiform and parahippocampal gyri that included the entorhinal and perirhinal cortices. Methodological differences between the studies could explain this discrepancy. We considered only gray matter in calculating the volume of the cortical areas, whereas Convit et al included the white matter in their volume estimations. Moreover, the cortical areas located caudal to the entorhinal and perirhinal cortices (ie, areas TH and TF) may also be damaged by aging, leading to a reduction in the total volume of the parahippocampal gyrus. Altogether, our data extend and clarify previous observations by demonstrating that the temporopolar cortex specifically, rather than the perirhinal or entorhinal cortices, is reduced with age.

The rate of cortical volume loss during the aging process is of interest. In a previous histologic study (24), the hemispheric volumes remained constant between 20 and 50 years of age. Thereafter, the volume decreased by approximately 2% per decade (24). These data support results from the MR imaging study of Coffey et al (25), who found approximately 0.23% volume loss per year in the cerebral hemispheres after the age of 30. The average age difference between the younger and older subjects in our study was 44 years, and the volume reduction in the temporopolar cortex was 13%. Therefore, if we assume that volume loss is linear over time, the volume of the temporopolar cortex reduces approximately 3% per decade. It is still a matter of dispute, however, whether the volume loss is due to the reduction of gray matter or white matter. Some studies indicate that brain shrinkage is almost exclusively due to loss of white matter (26). Other histologic and MR studies further the argument that cerebral volume reduction is primarily due to the loss of gray matter (24, 27, 28), which is supported by our analyses, in which only gray matter was included in the volumetric measurements.

Effect of Gender on Cortical Volumes

We did not observe any differences between men and women in the normalized volumes of the entorhinal, perirhinal, or temporopolar cortices. The combined perirhinal/temporopolar volume, however, was larger in women than in men. The raw volume of the hippocampus and the total volume of the temporal lobe have been found to be 11% and 16% smaller in females than in males, respectively (29), although this difference may be associated with variability in brain size, since this gender difference is eliminated once volumes are normalized according to head size (24, 29, 30). Moreover, aging may have different effects on temporal lobe regions in males and females (31, 32). In the present study, we did not find any gender-dependent effect of aging on the volumes of the entorhinal, perirhinal, and temporopolar cortices.

Hemispheric Asymmetry

The right entorhinal cortex was larger than the left. Several previous studies have reported the right hippocampus to be bigger than the left (14, 16, 33–36), although other studies have not confirmed this asymmetry (37–39). Moreover, the right amygdala was found to be larger than the left (16, 40), and Jack et al (33, 34) reported that the total temporal lobe volume and the anterior temporal lobe volume were larger in the right hemisphere than in the left. Opposing that, we found that the combined volume of the perirhinal and temporopolar cortices, which form most of the medial aspect of the anterior temporal lobe, was larger in the left hemisphere than in the right.

Functional Aspects

In addition to the hippocampus and the TH and TF parahippocampal areas, the entorhinal and perirhinal cortices are elementary components of the medial temporal lobe memory system (3). Damage to these regions causes impairment of memories of facts and events (4, 5, 41). Histopathologic studies have demonstrated damage to the entorhinal and perirhinal cortices in such disorders as Alzheimer disease (42, 43) and temporal lobe epilepsy (44), which in part may explain the memory impairment commonly associated with these disorders. It is unclear whether damage to medial temporal lobe cortical areas also contributes to memory impairment.

Conclusion

The MR-volumetric protocol described here provides a useful tool by which to measure the volumes of the entorhinal, perirhinal, and temporopolar cortices in living, awake humans. It may also be used to investigate the contribution of various medial temporal lobe cortical areas to normal cognitive processing. Furthermore, the appearance and progression of damage in various portions of the medial temporal cortex in conditions such as Alzheimer's disease or temporal lobe epilepsy may be more accurately quantified in patients by means of this technique.

References

1. Insausti R, Amaral DG, Cowan WM. **The entorhinal cortex of the monkey, II: cortical afferents.** *J Comp Neurol* 1987;264:356–395
2. Suzuki WA, Amaral DG. **Topographic organization of the reciprocal connections between the monkey entorhinal cortex and the perirhinal and parahippocampal cortices.** *J Neurosci* 1994; 14:1856–1877
3. Squire LR, Zola-Morgan S. **The medial temporal lobe memory system.** *Science* 1991;253:1380–1386
4. Suzuki WA, Zola-Morgan S, Squire LR, Amaral DG. **Lesions of the perirhinal and parahippocampal cortices in the monkey produce long-lasting memory impairment in the visual and tactual modalities.** *J Neurosci* 1993;13:2430–2451
5. Zola-Morgan S, Squire LR, Ramus SJ. **Severity of memory impairment in monkeys as a function of locus and extent of damage within the medial temporal lobe memory system.** *Hippocampus* 1994;4: 483–495
6. Alvarez P, Zola-Morgan S, Squire LR. **Damage limited to the hippocampal region produces long-lasting memory impairment in monkeys.** *J Neurosci* 15:3796–3807
7. Leonard BW, Amaral DG, Squire LR, Zola-Morgan S. **Transient memory impairment in monkeys with bilateral lesions of the entorhinal cortex.** *J Neurosci* 1995;15:5637–5659
8. Brodmann K. ***Vergleichende Lokalisationslehre der Grosshirnrinde in ihren Prinzipien dargestellet auf Grund des Zellenbaues.*** Leipzig: Barth, 1909
9. Insausti R, Tunon T, Sobreviela T, et al. **The human entorhinal cortex: a cytoarchitectonic analysis.** *J Comp Neurol* 1995;335:171–198
10. Amaral DG, Insausti R. **The human hippocampal formation.** In: Paxinos G, ed. *The Human Nervous System.* San Diego: Academic Press; 1990:711–755
11. Suzuki WA, Amaral DG. **Perirhinal and parahippocampal cortices of the macaque monkey: cortical afferents.** *J Comp Neurol* 1994; 350:497–533
12. Von Bonin G, Bailey P. ***The Neocortex of Macaca Mulatta.*** Urbana, Ill: University of Illinois Press; 1947
13. Pearlson GD, Harris GJ, Powers RE, et al. **Quantitative changes in mesial temporal volume, regional cerebral blood flow, and cognition in Alzheimer's disease.** *Arch Gen Psychiatry* 1992;49:402–408
14. Soininen HS, Partanen K, Pitkänen A, et al. **Volumetric MRI analysis of the amygdala and the hippocampus in subjects with age-associated memory impairment.** *Neurology* 1994;44:1660–1668
15. Free SL, Bergin PS, Fish DR, et al. **Methods for normalization of hippocampal volumes measured with MR.** *AJNR Am J Neuroradiol* 1995;16:637–643
16. Watson C, Andermann F, Gloor P, et al. **Anatomic basis of amygdaloid and hippocampal volume measurement by magnetic resonance imaging.** *Neurology* 1992;42:1743–1750
17. Sullivan EV, Marsh L, Mathalon DH, et al. **Age-related decline in MRI volumes of temporal lobe gray matter but not hippocampus.** *Neurobiol Aging* 1995;16:591–606
18. Kesslak JP, Nalcioglu O, Cotman CW. **Quantification of magnetic resonance scans for hippocampal and parahippocampal atrophy in Alzheimer's disease.** *Neurology* 1991;41:51–54
19. Shenton ME, Kikinis R, Jolesz FA, et al. **Abnormalities of the temporal lobe and thought disorder in schizophrenia: a quantitative magnetic resonance imaging study.** *N Engl J Med* 1992;327: 604–612
20. Erkinjuntti T, Lee DH, Gao F, et al. **Temporal lobe atrophy on magnetic resonance imaging in the diagnosis of early Alzheimer's disease.** *Arch Neurol* 1993;50:305–310
21. Nestor PG, Shenton Me, McCarley RW, et al. **Neuropsychological correlates of MRI temporal lobe abnormalities in schizophrenia.** *Am J Psychiatry* 1993;150:1849–1855
22. Gómez-Isla T, Price JL, McKeel DW Jr, et al. **Profound loss of layer II entorhinal cortex neurons occurs in very mild Alzheimer's disease.** *J Neurosci* 1996;16:4491–4500
23. Convit A, De Leon MJ, Hoptman MJ, et al. I. **Magnetic resonance imaging measures of temporal lobe volumes in normal subjects.** *Psychiatr Q* 1995;66:343–355
24. Miller AKH, Alston RL, Corsellis JAN. **Variation with age in the volumes of gray and white matter in the cerebral hemispheres of man: measurements with an image analyzer.** *Neuropathol Appl Neurol* 1980;6:119–132
25. Coffey CE, Wilkinson WE, Parashos IA, et al. **Quantitative cerebral anatomy of the aging human brain.** *Neurology* 1992;42:527–536
26. Albert M. **Neuropsychological and neurophysiological changes in healthy adult humans across the age range.** *Neurobiol Aging* 1993; 14:623–625
27. Lim KO, Zipursky RB, Watts MC, Pfefferbaum A. **Decreased gray matter in normal aging: an in vivo magnetic resonance study.** *J Gerontol* 1992;47:26–30
28. Pfefferbaum A, Mathalon DH, Sullivan EV, et al. **A quantitative magnetic resonance imaging study of changes in brain morphology from infancy to late adulthood.** *Arch Neurol* 1994;51:874–887
29. Bhatia S, Bookheimer SY, Gaillard WD, Theodore WH. **Measurement of whole temporal lobe and hippocampus for MR volumetry: normative data.** *Neurology* 1993;43:2006–2010
30. Gur RC, Mozley PD, Resnick SM, et al. **Gender differences in age effect on brain atrophy measured by magnetic resonance imaging.** *Proc Natl Acad Sci* 1991;88:2845–2849
31. Colomb J, De Leon MJ, Kluger A, et al. **Hippocampal atrophy in normal aging: an association with recent memory impairment.** *Arch Neurol* 1993;50:967–973
32. Colomb J, Kluger A, De Leon MJ, et al. **Hippocampal formation size in normal human aging: A correlate of delayed secondary memory performance.** *Learning Memory* 1994;1:45–54
33. Jack CR, Gehring DG, Sharbrough FW, et al. **Temporal lobe volume measurement from MR images: accuracy and left-right asymmetry in normal persons.** *J Comput Assist Tomogr* 1988;12: 21–29
34. Jack CR, Twomey CK, Marsh WR, et al. **Anterior temporal lobes and hippocampal formations: normative volumetric measurements from MR images in young adults.** *Radiology* 1989;172: 549–554
35. Jack CR, Sharbrough FW, Twomey CK, et al. **Temporal lobe seizures: lateralization with MR volume measurements of the hippocampal formation.** *Radiology* 1990;175:423–429
36. Cascino GD, Jack CR, Parisi JE, et al. **Magnetic resonance imaging-based studies in temporal lobe epilepsy: pathological correlations.** *Ann Neurol* 1991;30:31–36
37. Lencz T, McCarthy G, Bronen R, et al. **Hippocampus in temporal lobe epilepsy: correlation of presurgical MRI volumetrics with postsurgical cell counts (abstract).** *Epilepsia* 1990;31:667–668
38. Scott T, McCarthy G, Sass K, et al. **Hippocampal and temporal lobe measurements as an index of memory impairment in pa-**

tients with temporal lobe epilepsy (abstract). *Epilepsia* 1990;31: 630
39. Cook MJ, Fish DR, Shorvon SD, et al. **Hippocampal volumetric and morphometric studies in frontal and temporal lobe epilepsy.** *Brain* 1992;115:1001–1015
40. Filipek PA, Richelme C, Kennedy DN, Caviness VS Jr. **The young adult human brain: an MRI-based morphometric analysis.** *Cereb Cortex* 1994;4:344–360
41. Zola-Morgan S, Squire LR, Amaral DG, Suzuki WA. **Lesions of perirhinal and parahippocampal cortex that spare the amygdala and hippocampal formation produce severe memory impairment.** *J Neurosci* 1989;9:4355–4370
42. Hyman BT, Damasio AR, VanHoesen GW, Barnes CL. **Alzheimer's disease: cell-specific pathology isolates the hippocampal formation.** *Science* 1984;298:83–95
43. Braak H, Braak E. **Neuropathological staging of Alzheimer-related changes.** *Acta Neuropathol* 1991;82:239–259
44. Du F, Whetsell WO Jr, Abou-Khalil B, et al. **Preferential neuronal loss in layer III of the entorhinal cortex in patients with temporal lobe epilepsy.** *Epilepsy Res* 1993;16:223–233